





Specific binding of D-Amino neuraminic acid to ganglioside studied in prostate cancer cells

Prostat kanseri hücreleri'nde D-Amino nöraminik asidin ganglioizid'e spesifik bağlanmasının çalışılması

Kenan Demir¹  Huseyin Aktug²  Gurkan Yigitturk³  Eda Acikgoz⁴ 
Gunnur Guler⁵  Hadi Rouhrazl⁶ 

¹ Department of Histology and Embryology, Samsun Training and Research Hospital, University of Health Sciences Türkiye, Samsun, Türkiye

² Department of Histology and Embryology, Faculty of Medicine, Ege University, Izmir, Türkiye

³ Department of Histology and Embryology, Faculty of Medicine, Mugla Sitki Kocman University, Mugla, Türkiye

⁴ Department of Histology and Embryology, Faculty of Medicine, Van Yuzuncu Yil University, Van, Türkiye

⁵ Department of Biomedical Engineering, Izmir University of Economics, Izmir, Türkiye

⁶ Department of Basic Oncology, Institute of Health Sciences, Ege University, Izmir, Türkiye

ABSTRACT

Aim: The aim of this study was to investigate the cellular binding site of human D-Amino Neuraminic Acid (KDN, 2-keto-3-deoxy-D-glycero-D-galacto-nononic acid). The KDN molecule is a member of the sialic acid family, and its expression increases in cancer cells. KDN has been shown to bind to Monosialodihexosyl Ganglioside (GM3) in trout sperm.

Materials and Methods: In this study, a prostate cancer cell line (DU145) was used. Each experimental group was divided into 3 groups: Control, Glucosylceramide synthase (GCS) enzyme inhibitor Genz-123346-treated, and GM3 synthesis inhibitor Triptolide-treated. Each group was stained using the immunocytochemical method for GM3, Disialosyllactosylceramide (GD3) and KDN. Fourier Transform Infrared (FTIR) Spectroscopy analysis was performed to elucidate the cellular changes after treatment.

Results: The group of non-treated number 1 cells stained positive with GM3, GD3 and KDN, and the GCS enzyme was blocked with the Genz-123346 group of number 2 cells stained positive only with KDN. Furthermore, the group of GD3 synthase inhibitor Triptolide treated number 3 cells stained positive with GM3 and KDN. FTIR measurements showed apoptotic characteristics with Triptolide, while Genz-123346 did not have a negative effect on cell viability. There was a reduction in sugar structures and the results obtained with immunocytochemical staining were reinforced with FTIR.

Conclusions: Determining the location of the bound KDN is important for the selection of new targets for cancer treatment research. KDN has been shown to be not inhibited by GM3 inhibition and GD3 inhibition. KDN can be on GM3 as well as connected to different places or can be free. In this study, it was demonstrated that it would not bind to any of the gangliosides in the pure GM or GD series.

Keywords: Ganglioside, Genz-123346, GM, KDN, prostate cancer, triptolide.

Corresponding author: Kenan Demir
Department of Histology and Embryology, Samsun Training and Research Hospital, University of Health Sciences
Türkiye, Samsun, Türkiye
E-mail: kenandemir@hotmail.com
Application date: 05.11.2022 Accepted: 07.12.2022

ÖZ

Amaç: Bu çalışmanın amacı, insan D-Amino Nöraminik Asid'inin (KDN, 2-keto-3-deoksi-D-glisero-D-galakto-nononik asit) hücresel bağlanma bölgesini araştırmaktır. KDN molekülü, sialik asit ailesinin bir üyesidir ve kanser hücrelerinde ekspresyonu artar. KDN'nin alabalık spermünde Monosialodihexosyl Gangliosid'e (GM3) bağlandığı gösterilmiştir.

Gereç ve Yöntem: Bu çalışmada bir prostat kanseri hücre dizisi (DU145) kullanıldı. Her deney grubu; Kontrol, Glukosilseramid sentaz (GCS) enzim inhibitörü Genz-123346 ile tedavi edilen ve GM3 sentez inhibitörü Triptolid ile tedavi edilen olmak üzere 3 gruba ayrıldı. Her grup, GM3, Disialosyllactosylceramide (GD3) ve KDN için immünohistokimyasal yöntem kullanılarak boyandı. Tedaviden sonra hücresel değişikliklerin sağlanması Fourier Transform Infrared (FTIR) Spektroskopi analizi ile yapıldı.

Bulgular: Tedavi edilmeyen 1 numaralı hücre grubu, GM3, GD3 ve KDN ile pozitif boyandı ve GCS enzimi, sadece KDN ile pozitif boyanan 2 numaralı hücrelerin Genz-123346 grubuyla bloke edildi. Ayrıca, GD3 sentaz inhibitörü Triptolide ile muamele edilmiş 3 numaralı hücre grubu, GM3 ve KDN ile pozitif boyandı. FTIR ölçümleri Triptolide ile apoptotik özellikler gösterirken, Genz-123346 hücre canlılığı üzerinde olumsuz bir etkiye sahip değildi. Şeker yapılarında azalma ortaya çıktı ve immünohistokimyasal boyama ile elde ettiğimiz sonuçlar FTIR ile pekiştirildi.

Sonuç: KDN'nin yerinin belirlenmesi, kanser tedavisi araştırmaları için yeni hedeflerin seçilmesi açısından önemlidir. KDN'nin GM3 inhibisyonu ve GD3 inhibisyonu tarafından inhibe edilmediği gösterilmiştir. KDN, GM3 üzerinde olabileceği gibi farklı yerlere de bağlanabilir veya serbest halde olabilir. Bu çalışmada yalnızca salt GM veya GD serisindeki gangliozidlerden herhangi birine bağlanmayacağı ortaya konulmuştur.

Anahtar Sözcükler: Gangliozid, Genz-123346, GM, KDN, prostat kanseri, triptolide.

INTRODUCTION

Malignant tumors consist of cancer cells with different morphological characteristics. Cancer cells express varying cell surface markers for each type of tumor and exhibit heterogeneous intratumoral populations with different proliferation capacities. This heterogeneity is due to genetic/epigenetic and microenvironmental differences, as well as to different levels of differentiation. In targeted cancer therapy, the identification of surface antigens, signaling pathways, genetic landscape, and intercellular connection complexes is very important. Differentially expressed novel proteins, carbohydrates, and lipid structures in cancer cells are promising targets for the development of new therapeutic strategies.

Recent studies have shown that various glycolipids play a role in cancer cell invasion, neovascularization, and immune escape during metastasis (1, 2). Blocking glycolipids such as GM3 and GM2 has been shown to reduce tumor cell metastasis and induce apoptosis in cancer cells (3). Gangliosides are glycosphingolipids containing sialic acid, and recently some cancers have shown anticancer effects by blocking ganglioside molecules (4).

Gangliosides are abundant in brain tissue, where they are 5-fold more common in gray matter compared to white matter. In extraneural tissues, the ganglioside content is lower than in the brain; and can be in relatively higher concentrations in the bone marrow, erythrocytes, intestine, liver, spleen and testes, kidney, and embryonic stem cells. Gangliosides may act as receptors for certain hormones and bacterial toxins (5). They are involved in cell adhesion/recognition processes, signal transduction, tissue growth, and differentiation. Their composition is known to change in different pathologies, including carcinogenesis (5). Gangliosides are involved in intracellular membrane structures such as the nuclear envelope (6). Defects in ganglioside metabolism due to genetic mutations in the lysosomal enzymes responsible for their degradation result in accumulation in the musculoskeletal system, liver, spleen, and central nervous system, leading to a group of diseases called sphingolipidosis (7).

Gangliosides are synthesized from ceramide and contain one or more sialic acid residues. The structure consists of a glycosphingolipid (ceramide and oligosaccharide) and one or more N-acetyl neuraminic acid residues. The synthesis of gangliosides begins with the conversion of

ceramide by GCS (glucosylceramide synthase) to glucosylceramide (Glc-Cer). Glucosylceramide is converted to lactosylceramide (Lac-Cer, Gal-Glc-Cer) by galactosyltransferase I. Monosialodihexosyl ganglioside (GM3) is synthesized from lactosylceramide by the GM3 synthase enzyme. Other gangliosides are synthesized by GM3. GM2 is synthesized from GM3 with the enzyme GalNac-T (B4GALNT1, Beta-1,4 N-acetyl galactosaminyl transferase 1), while disialosyllactosylceramide (GD3) is synthesized from GM3 by GD3S (GD3 synthase, Alpha-N-acetyl neuraminidase alpha-2,8-sialyl transferase). GM2 is synthesized from GM3 and GM1 from GM2. GM3 is the key molecule for the synthesis of other gangliosides (8). In several studies, GM3 synthesis, namely all gangliosides, has been shown to be successfully inhibited by various molecules during the conversion from ceramide in the GCS step (9). The main molecules used in enzyme inhibition are Genz-123346, PPPP, PMPP, PDMP, NB-DNJ (N-butyl-deoxynojirimycin) and Genz-529468 (9). GD3 synthesis by GD3 synthase can be blocked by Triptolide (1).

2-Keto-3-deoxy-D-glycero-D-galacto-nonanic acid (KDN, D-aminoneuraminic acid) is considered a member of the sialic acid family with unique characteristics. KDN is formed by adding a hydroxyl group to position C5 in common Sia, instead of the aceto-amide group. KDN has different properties, including insensitivity to various sialidases and a "stop signal" for the prolongation of polysialic acid. In mammalian cells, KDN is often expressed at very low levels. It was first isolated by Inoue et al. as a polysialo-glycoprotein (10). The KDN molecule is synthesized by two separate pathways: 1) synthesis by deacetylation from Neu5Ac; and 2) de novo synthesis by different enzymes. KDN is found in many animals, from bacteria to high vertebrates, including humans. To date, KDN has been shown in the trout spore based on GM3 (11). No further studies have been conducted on KDN. The putative role of KDN in cancer can be demonstrated by the elucidation of its chemical structure. The aim of this study was to demonstrate whether KDN is associated only with GM series gangliosides.

MATERIALS and METHODS

Cell culture

A prostate cancer cell line (DU145) was obtained from the American Type Culture Collection (ATCC). RPMI 1640 medium was used for the growth and maintenance of the DU145 cell line.

1% penicillin / streptomycin, 10% heat inactivated fetal bovine serum, 1% amphotericin B and 1% L-glutamine were added to RPMI 1640 medium. All cells were grown at 37°C, 5% CO₂. The cell line was monitored daily in terms of viability, proliferation, and infection using an inverted microscope. When more than 80% cell density was observed, cells were propagated by passaging.

Cell Count and Viability Assay

Cell viability after treatment was determined using the Muse™ Count and Viability Kit (Muse™ Cell Analyzer; Millipore, Billerica, MA, USA) according to the manufacturer's instructions. Briefly, cells were seeded in triplicate in 6-well plates at a density of 1×10^4 cells/well. After 24 hours of incubation, cells were exposed to increasing concentrations of Genz-123346 (10, 100, 1000 nM) and Triptolide (20, 40, 60 nM). Then, the plates were incubated at 37°C in a 5% CO₂ incubator for 24, 48, and 72 hours. After incubation, all cells were collected and diluted with phosphate buffered saline (PBS). 50 µl of cell suspension was then added to the 450 µl Muse Count and Viability reagent (10x dilution), incubated for 5 minutes at room temperature, and analyzed using the Muse Cell Analyzer. Data were presented as proportional viability (%) by comparing the treated group with untreated cells, of which it is assumed that viability is 100%.

Immunocytochemical Staining

Cells were placed on coverslips and fixed with 4% paraformaldehyde for 30 minutes at 4°C and permeabilized with 0.01% Triton X-100 for 15 minutes at room temperature. Cells were blocked with serum blocking solution (Invitrogen, USA) for 30 minutes and incubated with primary antibodies (dilution of 1:100, at 4°C overnight), Anti-KDN antibody, Anti-Ganglioside GD3 antibody (ab11779) and Anti-GM3 Monoclonal antibody (AMS.A2582) in a humidity chamber. After washing with PBS, cells were incubated with a secondary antibody and streptavidin complex for 30 minutes. Substrate solution (DAB) (Invitrogen, USA) was applied and then, Mayer's hematoxylin was used for counterstaining. The immunoreactivity of the molecules was evaluated by light microscopy using Olympus BX-51 and C-5050 digital cameras.

Fourier Transform Infrared (FTIR) Spectroscopy

i. Sample Preparation

Cells were grown in T25 flasks. Cells were treated separately with the GCS inhibitor Genz-123346 at 1000 nM for 24 hours and the GD3S

inhibitor Triptolide at a dose of 60 nM for 72 hours. Before cell harvesting, the medium was discarded and the cells were rapidly washed with 1 ml of 0.05% trypsin (Sigma-Aldrich) to remove dead cell debris. Cells were then removed from their culture support, applying a 5 minute treatment with 1 ml of trypsin buffer at 37°C in a 5% CO₂ environment. The reaction was stopped by rinsing cells with 5 ml of culture medium with 10% FBS (fetal bovine serum). Cells were pelleted by 2 minute centrifugation (300 g), and washed three times with sterile isotonic solution (NaCl, 0.9%) to ensure complete removal of trypsin and culture medium. Finally, the cells were then resuspended in NaCl solution for ATR-FTIR analysis. Three independent cultures of four different conditions were grown for each condition, as given below.

- DU145 (untreated prostate cancer cell lines, called the control group)
- DU145 + Genz (Genz-treated prostate cancer cells)
- DU145 + Triptolide (Triptolide-treated prostate cancer cells)

ii. *ATR-FTIR Spectroscopy Measurements*

Measurements were made with an IRTracer-100 FTIR spectrometer (Shimadzu, Japan) combined with an attenuated total reflection (ATR) unit equipped with a DLATGS detector, as described in our previous studies (12, 13, 14). After placing a 2 µl amount of cell suspension (~1×10⁶ cell/ml) was placed on the ATR, it was evaporated for ~12 minutes to remove excess water from the cell suspensions. A total of 128 scans were averaged for each interferogram at a spectral resolution of 4 cm⁻¹ spectral resolution. The air spectrum was recorded as a background spectrum in the absence of a cell sample when the ATR plate was empty. Three samples were taken from each condition, so measurements were taken in triplicate. A minimum of four spectra per measurement were recorded in the range of 4.000 to 800 cm⁻¹.

iii. *FTIR Data Processing*

Spectral preprocessing, FTIR difference spectra and Student's t-tests were performed using the software 'Kinetics' running under MATLAB, as described in detail in our previous studies (12, 13, 14).

Spectral Preprocessing – After the IR spectra were recorded with LabSolutions software (Shimadzu, Japan), the spectral preprocessing and visualization of the data were performed with the *Kinetics* program. The all-recorded spectra

for each cell condition at different times should be comparable; thus these data require preprocessing prior to further data analysis (using the difference spectrum, mean spectrum, etc.). Consequently, first, the contribution of atmospheric water vapor in the IR spectra was subtracted by taking 1562–1555 cm⁻¹ as the reference peak. Subsequently, the straight lines were interpolated between the points of the spectrum at multiple wavenumbers. Then they were subtracted from the spectrum for baseline correction. After baseline correction, the spectra were normalized for an equal area between 1582 and 1482 cm⁻¹. Thus, the absorbance scale displays the rescaled absorbance values in figures. The 'mean' absorbance spectrum was also calculated for each cell condition by averaging the (baseline corrected and normalized) all-recorded spectra for triplicate experiments for each cell condition (grown independently). This was called the 'mean' in the present work.

Infrared Difference Spectra and Student's t-test –

The difference spectra were calculated using the mean absorbance spectra. For this purpose, the mean absorbance spectrum of 'untreated control DU145 cells' was subtracted from the mean absorbance spectrum of 'treated cells with Genz (or with Triptolide)', represented as follows: $\Delta A = (\text{treated}) - \text{minus} - (\text{untreated})$. Student's t-test was also employed at every wavenumber, allowing for a statistical comparison between the spectra of each cell condition. Herein, the red points demonstrate the wave numbers where there is a significant difference exists with a significance $\alpha=0.1\%$.

RESULTS

Cytotoxic Effects of Drugs

Our purpose in Muse analysis is to find the IC-50 value of the drugs (GCS Inhibitor Genz-123346 and GD3S Inhibitor Triptolide) used in the present study.

The effect of the GCS inhibitor on cell viability in DU145 cells was studied by applying the increased dose (at 10-1000 nM) and the time (at 24, 48 and 72 hours).

At the end of 24, 48 and 72 hours of GCS inhibitor treatment, no significant cytotoxic effects were determined in the dose range of 10-1000 nM in the DU145 cell line compared to the control. Genz-123346 was not cytotoxic to cells. At the end of 72 hours, 95.9% of the DU145 cell line was found to be in the 1000 nM Genz dose.

As a result, the IC-50 value of Genz-123346 was not found in the DU145 cell line. The cytotoxic effect of Genz-123346 concentrations of 10, 100 and 1000 nM in the DU145 cell line (at 24, 48 and 72 hours) at various times (24, 48 and 72 hours) was not statistically significant (Figure-1a). The effect of the GM3 inhibitor on DU145 cell viability was also investigated with respect to both the increased dose (20-60 nM) and the time (24, 48 and 72 hours).

After 24, 48 and 72 hours of treatment with the GM3 inhibitor, a significant cytotoxic effect was determined in the DU145 cell line when Triptolide concentrations of 20-60 nM were compared with the control group. At the end of 72 hours, the IC-50 values were determined as a 60 nM dose of Triptolide. The cytotoxic effect of Triptolide concentrations of 20, 40 and 60 nM on the DU145 cell line of the GD3S inhibitor (24, 48 and 72 hours) was found to be statistically significant (Figure-1b).

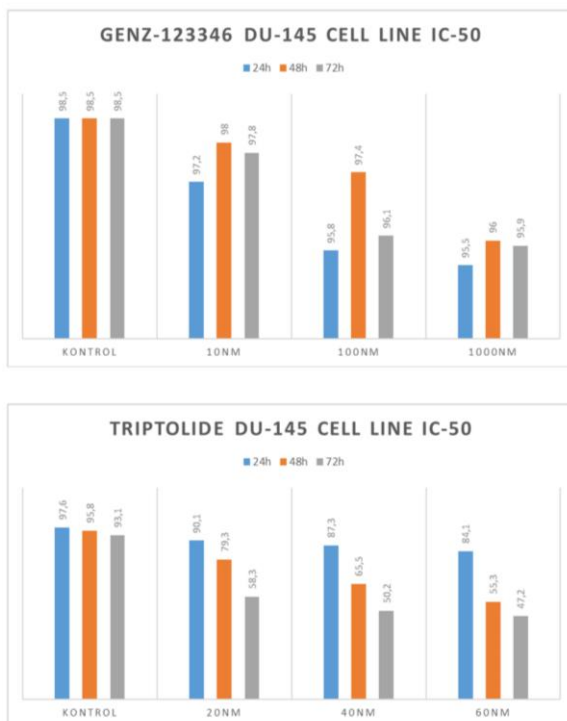


Figure-1 a. Effects of the GCS inhibitor Genz-123346 on cell viability, the DU145 cell line on cell viability at 24, 48 and 72 hours **b.** Effects of the GD3S inhibitor Triptolide on cell viability at 24, 48 and 72 hours in the DU145 prostate cancer cell line.

Immunocytochemical Staining

GCS Inhibitor Genz-123346 Treated Cell Lines

Changes of GM3, GD3 and KDN in cell lines treated with the GCS inhibitor were determined by the immunocytochemistry staining method. Cells were treated with the GCS inhibitor at 1000 nM for 24 hours. The GCS inhibitor was not added to the control group. Compared to the control group without a GCS inhibitor, a significant decrease in immunocytochemical staining with GM3 and GD3 antibodies was observed in the DU145 cell line after Genz-123346 staining (Figure-2).

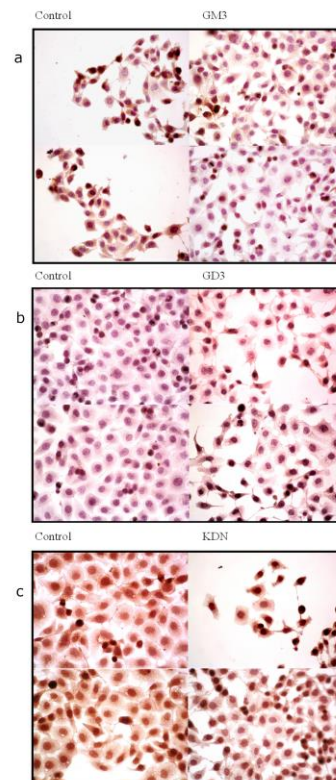


Figure-2 GCS inhibitor Genz-123346 treated with a 1000 nM dose for 24 hours. In the DU145 cell line, **a.** GM3 ganglioside, **b.** GD3 ganglioside and **c.** Light microscopic image of the change in KDN (40X)

Although Genz-123346 inhibited GM3 and GD3 gangliosides, KDN was not inhibited.

GM3S Inhibitor Triptolide Treated Cell Lines

Changes in GM3, GD3, and KDN in DU145 cell lines treated with a GD3S inhibitor were determined by the immunocytochemistry staining method. Cells were treated with a GD3S inhibitor at a dose of 60 nM for 72 hours. No GM3 inhibitor

was added to the control group. There was a significant decrease in GD3 in immunocytochemical staining after Triptolide in the DU145 cell line compared to the control group without a GM3 inhibitor (Figure-3).

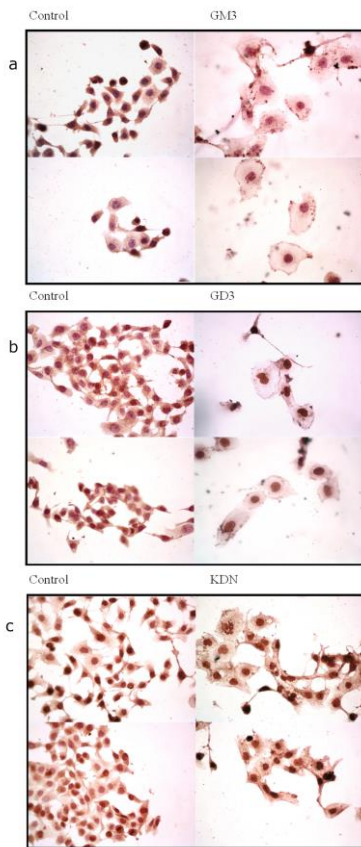


Figure-3. Treatment of the GD3S inhibitor Triptolide by 72 nM for 72 hours. DU145 cell line **a.** GM3 ganglioside **b.** GD3 ganglioside and **c.** Light microscopic image of the change in KDN (40X)

GM3 ganglioside and KDN were not inhibited despite inhibition of GD3 ganglioside in ICC staining with the GD3S inhibitor Triptolide.

FTIR spectroscopy results

Our main purpose in the FTIR analysis is to examine the effects of the drug on cellular molecules (protein, lipid, carbohydrate, and nucleic acid) in prostate cancer cells. Apoptotic spectral characteristics were not observed by the application of Genz-123346 in the DU145 prostate cancer cell line. Therefore, only changes due to GM3 blockade were observed. An increase in the α -helical proteins (1656 and 1549 cm^{-1}) was detected in the prostate cancer cell line after Genz-123346 treatment (the Amide I and

Amide II bands have positive absorbance peaks). A greater increase in lipid signals was observed in the case of Genz administration compared to Triptolide administration (unsaturated $=\text{CH}$ at 3011 cm^{-1} , saturated CH_2 at 2922 and 2853 cm^{-1} , CH_2 bend at 1460 cm^{-1} and $\text{C}=\text{O}$ stretch at 1745 cm^{-1}) (for band assignments, see ref [15, 16]). In our study, both the sialic acid signals (1118, 1044 and 1011 cm^{-1}) and the carbohydrate (sugar derivatives) signals (the $\text{C}-\text{O}$ stretching and $\text{C}-\text{O}-\text{H}$ bending modes of glycosidic bonds at 1150-950 cm^{-1}) were also decreased (Figures 4a, 4b) (for band assignments, see ref. [17, 18]).

Regular secondary structures of prostate cancer cell line proteins were reduced upon application of Triptolide to the DU145 cell line (the Amide I and Amide II bands have negative absorbances): protein α -helix structures (1659 cm^{-1}) decreased while the β -sheets (1629 cm^{-1}) increased. This strongly suggests that apoptosis occurs in the cell line after treatment.

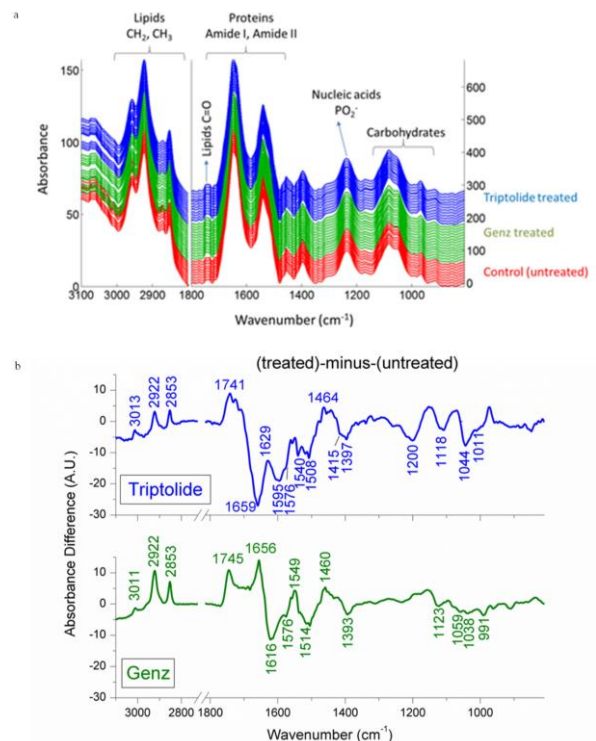


Figure-4 a. A series of FTIR spectra for DU145 human prostate cancer cells treated with control, Genz-123346, and Triptolide in the spectral region of 3100-2800 and 1800-800 cm^{-1} . **b.** The FTIR difference spectra (obtained from Figure 4a). All FTIR data administered by Triptolide and Genz-123346 were shown in the ranges of 3100-2800 cm^{-1} and 1800-800 cm^{-1} . The spectra were corrected for baseline and normalized to the amide II band.

After Triptolide treatment, an increase in lipid signals was also observed (unsaturated =CH at 3013 cm^{-1} , saturated CH_2 at 2922 and 2853 cm^{-1} , CH_2 bending at 1464 cm^{-1} , and C=O stretching at 1741 cm^{-1}). This spectrum is most likely due to changes in the plasma membrane induced by apoptosis, which also result in reductions in gangliosides, sugar derivatives (oligosaccharides and monosaccharides), and sialic acids. Carbohydrate (sugar derivatives) signals (1180-900 cm^{-1}) and sialic acid signals (1118, 1044 and 1011 cm^{-1}) decreased significantly as well (Figures-4a, 4b).

The FTIR results support the immunocytochemical staining results obtained here.

DISCUSSION

Cancer cells use gangliosides and some other glycolipids to induce angiogenesis, invasion, metastasis, and escape the immune system (1, 2).

Blocking glycolipids has been tried as a treatment and blocking some glycolipids has been shown to reduce tumor cell metastases and has even been found to lead cancer cells to apoptosis (3). Genz-123346 has been used in some studies to inhibit GCS (19, 20).

In 2010, in the study by Natoli and Karman, mice were treated with Genz-123346. The study showed the effects of the treated mice' kidneys. This *in vivo* study showed that both GSC and GM3 were reduced using immunohistochemical and Western blot methods with Genz-123346 (20). Karman has found the same result when using the Western blot method in the mouse lung (19). Similar results were obtained in the culture of the human prostate cancer cell line DU145 in our study. In the study by Haw-Young Kwon, the inhibition of GD3 by Triptolide was demonstrated by a decrease in the expression of the hST8Sia I gene in SK-MEL-2 human melanoma cells (21). In our study, the inhibition of GD3S in the DU145 cell line by Triptolide was demonstrated by immunocytochemical staining and FTIR spectroscopy. Song Yu showed the relationship between KDN and GM3 using thin layer chromatography (TLC), Western Blot, and immunoelectron microscopy (11).

In our study, we wanted to determine whether or not KDN is specifically associated with GM3. However, according to immunocytochemical staining and FTIR results, we did not reject a GM3 relationship, but it was revealed that it would not be possible to talk about GM3

specifically. Increased levels of gangliosides can be used to assess tumor prognosis in patients with bladder cancer (22). In a study, the association of the GD3 ganglioside with Snail, Twist, and TGF- β 1 in epithelio-mesenchymal transition and metastasis in breast cancer was demonstrated. In *in vitro* SUM159 and MDA-MB-231 in the study of cell lines, GD3 is required for wound healing, invasion, and stem cell function. In *in vivo* mouse studies, inhibition of GD3S inhibits metastasis (2). GM3 ganglioside has been shown to be related to Cisplatin-induced apoptosis in human colon cancer. It has been found that in the reduction of GM3 synthase with siRNA, and therefore all other gangliosides, especially GM3, precursors protect HCT116 human colon carcinoma cells from Cisplatin-mediated apoptosis, and apoptotic signal pathways due to free oxygen radical damage, such as Bax, Bcl-2, and p53, have been shown to be inhibited (4).

In the FTIR analysis, apoptosis was not observed with the administration of Genz-123346. Therefore, only changes due to GM3 blockade were observed. In the prostate cancer cell line, α -helix structural proteins were observed to increase at 1656 and 1549 cm^{-1} (the Amide I and Amide II bands have positive absorbances). Lipoprotein signals show a greater increase compared to Triptolide application (unsaturated =CH at 3011 cm^{-1} , saturated CH_2 at 2922 and 2853 cm^{-1} , CH_2 bending 1460 cm^{-1} , and C=O at 1745 cm^{-1}). This sequence of spectra reflects the exposure of lipid fatty acids to the cell surface as a consequence of the reduction in gangliosides and sugar derivatives (oligosaccharides, monosaccharides) and sialic acids on the extracellular surface after Genz-123346 treatment, which blocks GM3 synthesis. This shows that the fatty acids of the plasma membrane are significantly uncovered. The reduction in the 1616 and 1514 cm^{-1} IR signal (arising from C-C bond vibrations of carbohydrates) is most likely due to the low amounts of carbohydrates, sugar derivatives, and sialic acids. Due to a significant reduction in the amount of negatively charged sialic acids after Genz treatment, negatively charged COO^- molecular group signals (1616-1576 and 1393 cm^{-1}) were also reduced.

In our study, it was shown that the carbohydrate signals (sugar derivatives) signals arising from the C-O stretching and C-O-H bending vibrations of glycosidic bonds absorbed at 1150-950 cm^{-1} (17), as well as the sialic acid signals (1118, 1044 and 1011 cm^{-1}) (18) also decreased.

When Triptolide is applied, the regular structures of prostate cancer cell line proteins are reduced. Protein α -helix structures decreased at 1659 cm^{-1} , while β -sheet structures increased at 1629 cm^{-1} (negative absorbance at the Amide I and Amide II bands). This strongly suggests that apoptosis occurs after treatment (23).

Due to the application of Triptolide, an increase in lipid signals is observed. Lipid signals increase at 3013 cm^{-1} (unsaturated =CH), 2922 and 2853 cm^{-1} (saturated CH_2), 1464 cm^{-1} (CH_2 bending mode) and 1741 cm^{-1} (ester C=O), respectively. This spectrum pattern is most likely due to the apoptosis-induced plasma membrane blebbing, which also results from the reduction of gangliosides, sugar derivatives (oligosaccharides, monosaccharides) and sialic acids. Negatively charged COO^- molecular group signals also decrease (1595 - 1576 and 1415 - 1397 cm^{-1}), probably due to a significant reduction in the amounts of negatively charged sialic acids and amino acids. In the spectral region between 1250 and 1200 cm^{-1} , the DNA phosphate groups (phosphodiester vibrations) give rise to peaks, and the decrease in this signal indicates that the IR signals from DNA are also reduced. This indicates DNA fragmentation due to apoptosis (24, 25).

In our study, the results of the FTIR analysis, the ICC staining results, and the Muse IC-50 results supported each other. Genz-123346 did not show any cytotoxic effect on cells and no IC-50 value was found in the Muse assay. The same result was demonstrated by showing that Genz-123346 did not induce apoptosis in the DU145 cell line

according to the FTIR analysis. In the Triptolide FTIR analysis, it was shown that the DU145 cell line underwent apoptosis and, with the result of the IC-50 study in the Muse assay, a compatible result has arisen. The reduction in the amount of sialic acid in the DU145 cell line by applying Genz and Triptolide in the FTIR analysis coincided with the ICC staining.

CONCLUSION

In this study, it was determined whether or not GDN is specifically dependent on GM3. However, according to the results of our immunocytochemical staining and FTIR analysis, GM3 does not reject the relationship, but it is not possible to mention any specific attachment to GM3. With the results of the study, KDN has not been shown on GM3, but has led to another discussion. KDN is present not only on GM3, but also in free or bound structures on cellular membranes. It cannot be concluded from this study that KDN is not present only on GM3, but it can be concluded that the location may be anywhere on the cell.

Conflict of interest: The authors declare that they have no conflict of interest.

Acknowledgements: FTIR measurements were performed at the Center for Drug Research & Development and Pharmacokinetic Applications (ARGEFAR), Ege University, Izmir. The authors thank Prof. Dr. Ercüment Karasulu for permission to use the FTIR spectrometer. The authors also thank Prof. Dr. Erik Goormaghtigh from Université Libre De Bruxelles, Belgium, for providing the *Kinetics* software.

References

1. Battula VL, Shi Y, Evans KW, Wang RY, Spaeth EL, Jacamo RO, et al. Ganglioside GD2 identifies breast cancer stem cells and promotes tumorigenesis. *J Clin Invest.* 2012;122(6):2066-78. <https://doi.org/10.1172/JCI59735>
2. Sarkar TR, Battula VL, Werden SJ, Vijay GV, Ramirez-Peña EQ, Taube JH, et al. GD3 synthase regulates epithelial-mesenchymal transition and metastasis in breast cancer. *Oncogene.* 2015;34(23):2958-67. <https://doi.org/10.1038/onc.2014.245>
3. Ponnapakam AP, Liu J, Bhinge KN, Drew BA, Wang TL, Antoon JW, et al. 3-Ketone-4,6-diene ceramide analogs exclusively induce apoptosis in chemo-resistant cancer cells. *Bioorg Med Chem.* 2014;22(4):1412-20. <https://doi.org/10.1016/j.bmc.2013.12.065>
4. Chung TW, Choi HJ, Kim SJ, Kwak CH, Song KH, Jin UH, et al. The ganglioside GM3 is associated with cisplatin-induced apoptosis in human colon cancer cells. *PLoS One.* 2014;9(5):e92786. <https://doi.org/10.1371/journal.pone.0092786>
5. Lehninger AL, David LN, Cox MM. Lipids. In: Lehninger AL, David LN (ed) *Lehninger Principles of Biochemistry*, New York: W.H. 2005:357. doi: 10.1007/978-3-662-08289-8
6. Ledeen RW, Wu G. GM1 ganglioside: another nuclear lipid that modulates nuclear calcium. GM1 potentiates the nuclear sodium-calcium exchanger. *Can J Physiol Pharmacol.* 2006;84(3-4):393-402. <https://doi.org/10.1139/y05-133>

7. Utz JR, Crutcher T, Schneider J, Sorgen P, Whitley CB. Biomarkers of central nervous system inflammation in infantile and juvenile gangliosidoses. *Mol Genet Metab.* 2015;114(2):274-80. <https://doi.org/10.1016/j.ymgme.2014.11.015>
8. Krengel U, Bousquet PA. Molecular recognition of gangliosides and their potential for cancer immunotherapies. *Front Immunol.* 2014;21:325. <https://doi.org/10.3389/fimmu.2014.00325>
9. Liu YY, Hill RA, Li YT. Ceramide glycosylation catalyzed by glucosylceramide synthase and cancer drug resistance. *Adv Cancer Res.* 2013;117:59-89. <https://doi.org/10.1016/B978-0-12-394274-6.00003-0>
10. Nadano D, Iwasaki M, Endo S, Kitajima K, Inoue S, Inoue YA. Naturally occurring deaminated neuraminic acid, 3-deoxy-D-glycero-D-galacto-nonulosonic acid (KDN). Its unique occurrence at the nonreducing ends of oligosialyl chains in polysialoglycoprotein of rainbow trout eggs. *J Biol Chem.* 1986;261(25):11550-7.
11. Yu S, Kojima N, Hakomori SI, Kudo S, Inoue S, Inoue Y. Binding of rainbow trout sperm to egg is mediated by strong carbohydrate-to-carbohydrate interaction between (KDN)GM3 (deaminated neuraminyl ganglioside) and Gg3-like epitope. *Proc Nat Acad Sci USA.* 2002;99(5):2854-9. <https://doi.org/10.1073/pnas.052707599>
12. Güler G, Acikgoz E, Karabay Yavasoglu NÜ, Bakan B, Goormaghtigh E, Aktug H. Deciphering the biochemical similarities and differences among mouse embryonic stem cells, somatic and cancer cells using ATR-FTIR spectroscopy. *Analyst.* 2018;143(7):1624-34. <https://doi.org/10.1039/c8an00017d>
13. Acikgoz E, Güler G, Camlar M, Oktem G, Aktug H. Glycogen synthase kinase-3 inhibition in glioblastoma multiforme cells induces apoptosis, cell cycle arrest and changing biomolecular structure. *Spectrochim Acta A Mol Biomol Spectrosc.* 2019;209:150-64. <https://doi.org/10.1016/j.saa.2018.10.036>
14. Güler G, Guven U, Oktem G. Characterization of CD133+/CD44+ human prostate cancer stem cells with ATR-FTIR spectroscopy. *Analyst.* 2019;144(6):2138-49. <https://doi.org/10.1039/C9AN00093C>
15. Barth A. Infrared spectroscopy of proteins. *BBA – Bioenergetics.* 2007;1767(9):1073-101. <https://doi.org/10.1016/j.bbabi.2007.06.004>
16. Güler G, Gärtner RM, Ziegler C, Mäntele W. Lipid-Protein Interactions in the Regulated Betaine Symporter BetP Probed by Infrared Spectroscopy. *J Biol Chem.* 2016;291(9):4295-307. <https://doi.org/10.1074/jbc.M114.621979>
17. Karman J, Tedstone JL, Gumlaw NK, Hu Y, Yew N, Siegel C, et al. Reducing glycosphingolipid biosynthesis in airway cells partially ameliorates disease manifestations in a mouse model of asthma. *Int Immunol.* 2010;22(7):593-603. <https://doi.org/10.1093/intimm/dxq044>
18. Natoli TA, Smith LA, Rogers KA, Wang B, Komarnitsky S, Budman Y, et al. Inhibition of glucosylceramide accumulation results in effective blockade of polycystic kidney disease in mouse models. *Nat Med.* 2010;16(7):788-92. <https://doi.org/10.1038/nm.2171>
19. Kwon HY, Kim SJ, Kim CH, Son SW, Kim KS, Lee JH, et al. Triptolide downregulates human GD3 synthase (hST8Sia I) gene expression in SK-MEL-2 human melanoma cells. *Exp Mol Med.* 2010;42(12):849-55. <https://doi.org/10.3858/em.2010.42.12.088>
20. Slevin M, Costello B, Kumar S, Gaffney J. The ganglioside GM(3) is raised in the sera and tissue of patients with bladder tumours. *Int J Oncol.* 1996;8(2):271-4. <https://doi.org/10.3892/ijo.8.2.271>
21. Kacuráková M, Mathlouthi M. FTIR and laser-Raman spectra of oligosaccharides in water: characterization of the glycosidic bond. *Carbohydr Res.* 1996;284(2):145-57. [https://doi.org/10.1016/0008-6215\(95\)00412-2](https://doi.org/10.1016/0008-6215(95)00412-2)
22. Lewis AT, Jones K, Lewis KE, Jones S, Lewis PD. Detection of Lewis Antigen Structural Change by FTIR Spectroscopy. *Carbohydr Polym.* 2013;92(2):1294-301. <https://doi.org/10.1016/j.carbpol.2012.09.078>
23. Le Roux K, Prinsloo LC, Meyer D. Fourier Transform Infrared spectroscopy discloses different types of cell death in flow cytometrically sorted cells. *Toxicol In Vitro.* 2015;29(7):1932-40. <https://doi.org/10.1016/j.tiv.2015.08.002>
24. Plaimee P, Weerapreeyakul N, Thumanu K, Tanthanuch W, Barusrux S. Melatonin induces apoptosis through biomolecular changes, in SK-LU-1 human lung adenocarcinoma cells. *Cell Prolif.* 2014;47(6):564-77. <https://doi.org/10.1111/cpr.12140>
25. Gao Y, Huo X, Dong L, et al. Fourier transform infrared microspectroscopy monitoring of 5-fluorouracil-induced apoptosis in SW620 colon cancer cells. *Mol Med Rep.* 2015;11(4):2585-91. <https://doi.org/10.3892/mmr.2014.3088>